Journal of Computational and Applied Mathematics 236 (2012) 4611–4622

Contents lists available at SciVerse ScienceDirect

Journal of Computational and Applied Mathematics

journal homepage: www.elsevier.com/locate/cam

An adaptive solar radiation numerical model

F. Díaz *, G. Montero, J.M. Escobar, E. Rodríguez, R. Montenegro

University Institute for Intelligent Systems and Numerical Applications in Engineering, University of Las Palmas de Gran Canaria, Edificio Central del Parque Tecnológico, Campus de Tafira, 35017, Las Palmas de Gran Canaria, Spain

ARTICLE INFO

Article history:
Received 26 June 2011
Received in revised form 16 April 2012

Keywords:
Solar radiation
Shadows
Adaptive meshes
Solar power

ABSTRACT

A numerical model for the evaluation of solar radiation in different locations is presented. The solar radiation model is implemented taking into account the terrain surface using two-dimensional adaptive meshes of triangles that are constructed using a refinement/derefinement procedure in accordance with the variations of terrain surface and albedo. The selected methodology defines the terrain characteristics with a minimum number of points so that the computational cost is reduced for a given accuracy. The model can be used in atmospheric sciences as well as in other fields such as electrical engineering, since it allows the user to find the optimal location for maximum power generation in photovoltaic or solar thermal power plants. For this purpose, the effect of shadows is considered in each time step. The solar radiation is first computed for clear sky conditions considering the different components of the radiation. The real sky radiation is computed daily, starting from the results of clear sky radiation, in terms of the clear sky index. Maps for the clear sky index are obtained from a spatial interpolation of observational data that are available for each day at several points of the region under consideration. Finally, the solar radiation maps for a month are calculated from the daily results. The model can also be applied in solar radiation forecasting with the help of a forecasting meteorological model. This model takes into account the shadows cast, and allows the user to make a better estimation of the amount of solar power generation. Some numerical experiments related to the generation of solar radiation maps in Gran Canaria Island (Canary Islands, Spain) are presented.

1. Introduction

Knowledge about solar radiation is relevant in meteorology, forestry, agronomy, geography, and medicine because it affects all physical, chemical, and biological processes. Moreover, determining the solar radiation values in any location is essential for solar power generation. Part of the research in this field is the development of solar radiation numerical models. These models need to take into account the interaction of the radiation with the terrestrial atmosphere and surface, as follows [1].

1. The geometry of the Earth (declination, latitude, solar hour angle).
2. The terrain characteristics (elevation, albedo, surface inclination and orientation, shadows).
3. The atmospheric attenuation (scattering, absorption) caused by gases, particles, and clouds.

When all the atmospheric attenuation factors are considered, the model will give real sky radiation values. However, if cloud attenuation is omitted, clear sky (cloudless) radiation values will be obtained.

* Corresponding author.
E-mail address: fdiaz@die.ulpgc.es (F. Díaz).

0377-0427/$ – see front matter © 2012 Elsevier B.V. All rights reserved.
doi:10.1016/j.cam.2012.04.018

Starting from the spatial model developed in [1], which is based on astrophysical, atmospheric, physical, and geometrical considerations, the calculation of solar radiation on the terrain [2,3] is studied. The factors related to the terrain such as the elevation, the albedo, the surface inclination, and the shadows cast, are essential to have a precise idea of how the radiation comes into contact with the surface. The shadowing effect over a surface has been studied in [4] and [5]. Since they use a regular grid in their computations, the computational cost of this approach is higher than others using an adaptive discretization.

In this paper, a solution for the estimation of the solar radiation on the terrain with a low computational cost is applied. An adaptive mesh of triangles [2,3] is used to represent the terrain and its actual orography as a solid surface that really casts shadows. Mesh refinement/derefinement techniques have been widely used in other scientific problems [6,7].

2. Modelling of shadows and terrain characteristics

2.1. Terrain surface mesh

As Montero et al. [2] described, an adaptive procedure of mesh refinement/derefinement has been carried out using two different derefinement parameters, one for the orography and one for the albedo. Although the problem requires the use of four variables, namely, the node coordinates, height, and albedo, in reality, the construction of the mesh is a two-dimensional problem.

Starting from a regular triangulation τ_1 of the rectangular region under study, a sequence of nested meshes $\Gamma = \{\tau_1 < \tau_2 < \cdots < \tau_m\}$ will be built. The triangulation is such that level τ_j is obtained by a global refinement of the previous level τ_{j-1} with the 4-T Rivara algorithm [8]. The number of levels m of the sequence is determined by the degree of discretization of the terrain, so we can ensure that this regular mesh is able to capture all the orographic and albedo information by an interpolation of the heights and albedo in the nodes of the mesh.

Once this is done, we have to define a new sequence $\Gamma' = \{\tau_1 < \tau'_2 < \cdots < \tau'_{m'}\}$, $m' \leq m$, by applying a derefinement algorithm [7]. By means of two derefinement parameters, ε_h and ε_a, we can determine the accuracy of the approximation with respect to the terrain surface and albedo, respectively. On the one hand, we consider the analysis of the absolute difference between the exact height of a node and the interpolated height corresponding to the two extreme nodes of its environment edge, i.e., the edge in which that node was inserted in the middle point during the refinement process. On the other hand, the same analysis is carried out with the albedo. If the first difference related to the height is lower than ε_h and the second difference related to the albedo is lower than ε_a, simultaneously, then the node may be eliminated, although in some cases it will have to be kept for reasons of conformity.

2.2. Detection of shadows

The accurate estimation of the solar radiation on a terrain surface needs to take into account the shadows cast. This problem is, after all, a geometrical one: a triangle will be shadowed when, looking at the mesh from the Sun, we can find another triangle that totally or partially covers the former.

One way to face this issue is by constructing a reference system x', y' and z', with z' in the direction of the beam radiation (see Fig. 1). After this is done, the mesh needs to be projected on the plane $x'y'$ to see, for each triangle, if there are any other triangles that are overlapped.

The Sun's position with respect to a horizontal surface is given by two coordinates, the solar altitude h_0 and the solar azimuth A_0 (see Fig. 1), which are calculated as

$$\sin h_0 = \cos\varphi \cos\delta \cos T + \sin\varphi \sin\delta \tag{1}$$

$$\cos A'_0 = \frac{\sin\varphi \cos\delta \cos T - \cos\varphi \sin\delta}{\sin h_0} \tag{2}$$

$$\text{if } \sin T > 0, \quad A_0 = -A'_0$$

$$\text{if } \sin T \leq 0, \quad A_0 = A'_0.$$

T is the hour angle (rad) obtained from Eq. (3), φ the latitude in radians, and δ the Sun's declination in radians, obtained according to Gruter [9]. The hour angle T (rad) is calculated from the local solar time t expressed in decimal hours on the 24 h clock as

$$T = \frac{\pi}{12}(t - 12). \tag{3}$$

As said above, we need to make a coordinate transformation to get z' in the direction of the beam radiation. Thus, we need to know a vector that defines the solar beam direction for any time and position. In the literature we can find many ways to obtain this. Blanco-Muriel et al. proposed the so-called PSA algorithm [10], developed at the Plataforma Solar de Almería.

Once the coordinates transformation is done, the intersection between triangles is checked. This analysis involves a high computational cost. To diminish this cost, we have considered four warning points for each triangle, as can be seen in Fig. 2,

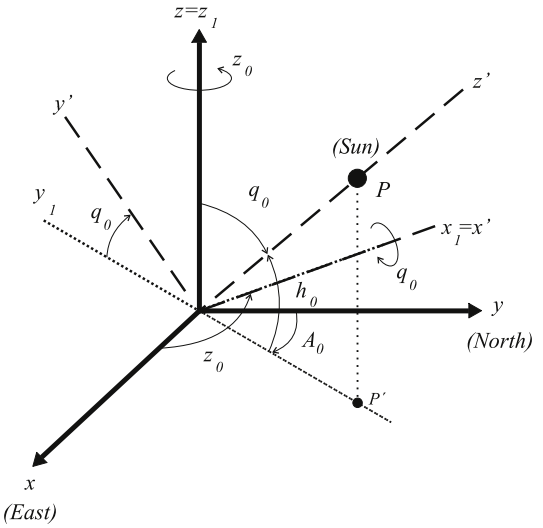

Fig. 1. Reference system and Euler angles.

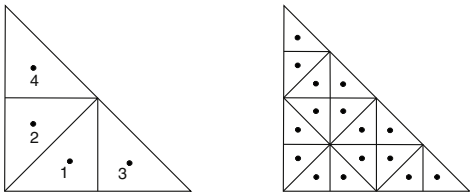

Fig. 2. Warning points for shading analysis.

left. This is not the only possibility, since we can, if needed, add more precision to the shade detection simply by increasing the number of warning points, as can be seen in Fig. 2 right, where now we have 16 warning points instead of the former four points.

We assign a different level of lighting or shade to each triangle of the mesh depending on the number of warning points that lie inside other triangles. Specifically, a triangle Δ will have an associated lighting factor which will be

$$L_f = \frac{n_{wp} - i}{n_{wp}}, \tag{4}$$

with $i = 0, 1, \ldots, n_{wp}$ being the number of warning points inside other triangles that are in front of Δ. Clearly, L_f is a quantity between 0 and 1. This factor is used below in the estimation of beam and diffuse irradiances.

3. Solar radiation modelling

Once the terrain is discretized by means of adaptive meshes, it is time to calculate the radiation values on every triangle. This will be done using a solar radiation model based on the works of Šúri and Hofierka [1]. The values are computed for each time step, taking into account the shadows over each triangle of the surface [2,3] using the method described above.

The results will be the clear sky irradiance values for each triangle. However, since the expected weather conditions have a tremendous influence on the probable radiation values that reach the surface, it is essential to take them into account. Considering the cloudiness and all the other atmospheric attenuation factors will lead us to obtain the real sky irradiance values. Therefore, the knowledge of some of the actual existing meteorological variables in the zone being studied is needed. A simple and accurate way to face this issue is using observational radiation data available from different measurement stations. A statistical analysis of the observational data is needed to get more accurate results about the values of real sky radiation that can be expected in a place at a certain time and date of the year. This analysis will give us a typical meteorological year (TMY) [11] that will be the starting point for converting the clear sky into real sky.

The calculation procedure would be as follows.

1. Solar radiation calculation for all the mesh, assuming clear sky conditions.
2. TMY calculation for all the measurement stations involved.
3. Correction of the solar radiation values using the measured values to reach the real sky conditions.

Steps one and three are repeated for each time step, and finally the total solar irradiation value is obtained integrating all the instantaneous values over a period of time.

3.1. Solar radiation equations for clear sky

The global solar irradiance comprises three different components: *beam*, *diffuse*, and *reflected* irradiances. The first component, though partially attenuated by the atmosphere, is not reflected or scattered, and reaches the surface directly. The second is the scattered irradiance that reaches the terrain surface and that goes in all directions and produces no shadows because of the opaque objects inserted. The third is the irradiance that is reflected from the surface onto an inclined receiver, and that depends on the ground albedo.

3.1.1. Beam radiation

According to Page [13], we will take the solar constant outside the atmosphere at the mean solar distance, I_0, as 1367 (W/m^2). Due to the eccentricity of the Earth's orbit, a correction factor ϵ is needed for the calculation of the extraterrestrial irradiance G_0.

$$G_0 = I_0\epsilon, \tag{5}$$

where ϵ depends on the day angle. The beam irradiance, normal to the solar beam, G_{b0} (W/m^2) is attenuated by the cloudless atmosphere, and is calculated as follows:

$$G_{b0c} = G_0 \exp\{-0.8662 T_{LK} m \delta_R(m)\}. \tag{6}$$

The term $0.8662T_{LK}$ is the dimensionless Linke atmospheric turbidity factor corrected in [14]. Subindex c shows that we are calculating clear sky irradiances. The parameter m in (6) is the relative optical air mass calculated as proposed in [15], and $\delta_R(m)$ is the Rayleigh optical thickness at air mass m.

Taking into account the above, the beam irradiance on a horizontal surface for clear sky conditions $G_{bc}(0)$ becomes

$$G_{bc}(0) = G_{b0c}\, L_f\, \sin h_0, \tag{7}$$

where h_0 is the solar altitude angle and L_f is the lighting factor that corrects the beam irradiance as the surface is sunlit or shadowed. The beam irradiance on an inclined surface for clear sky conditions $G_{bc}(\beta)$ is obtained as

$$G_{bc}(\beta) = G_{b0c} L_f \sin \delta_{\exp}, \tag{8}$$

where β is the angle between the inclined surface and the horizontal, and $\delta_{\exp}$ is the solar incidence angle measured between the sunbeam direction and its projection on an inclined surface.

3.1.2. Diffuse radiation

The estimation of the diffuse component in horizontal surfaces $G_{dc}(0)$ (W/m^2) is carried out using the equation

$$G_{dc}(0) = G_0 T_n(T_{LK}) F_d(h_0). \tag{9}$$

As can be seen, $G_{dc}(0)$ is a function of the diffuse transmission T_n which, at the same time, depends on the Linke turbidity factor T_{LK}. Also, we have the function F_d, which depends on the solar altitude h_0 [16]. To obtain the diffuse irradiance on a inclined surface, $G_{dc}(\gamma_N)$, with γ_N being the angle between the normal to a triangle and the horizontal plane, both sunlit and shadowed surfaces have to be considered using the equations proposed in [17].

3.1.3. Reflected radiation

The last component to take into account is the ground reflected irradiance under clear sky conditions ($G_r(\gamma_N)$). According to Muneer [18], this will be proportional to the global horizontal irradiance $G_c(0)$, to the mean ground albedo ρ_g, and to the fraction of the ground viewed by an inclined surface $r_g(\gamma_N)$.

$$G_r(\gamma_N) = \rho_g G_c(0) r_g(\gamma_N), \tag{10}$$

where

$$r_g(\gamma_N) = (1 - \cos \gamma_N)/2 \tag{11}$$

$$G_c(0) = G_{bc}(0) + G_{dc}(0). \tag{12}$$

3.2. Real sky solar radiation

The values of global radiation on a horizontal surface for real sky conditions $G(0)$ are calculated as a correction of those of clear sky $G_c(0)$ with the clear sky index k_c:

$$G(0) = G_c(0) k_c. \tag{13}$$

As k_c values are known for all the measurement stations, the next step will be the interpolation of the index for the whole zone. A simple formula that has also been used in other environmental problems defined on complex orography [19] is applied:

$$k_c = \varepsilon \frac{\sum_{n=1}^{N} \frac{k_{cn}}{d_n^2}}{\sum_{n=1}^{N} \frac{1}{d_n^2}} + (1-\varepsilon) \frac{\sum_{n=1}^{N} \frac{k_{cn}}{|\Delta h_n|}}{\sum_{n=1}^{N} \frac{1}{|\Delta h_n|}}, \tag{14}$$

where k_c corresponds to the clear sky index at each point of the mesh, k_{cn} is the clear sky index obtained at the measurement stations, N is the number of stations used in the interpolation, d_n is the horizontal distance and $|\Delta h_n|$ is the difference in height between station n and the point studied, respectively, and ε is a parameter between 0 and 1. In problems with regular orography, we choose high values of ε. However, for complex terrains, lower values of ε are a better choice. Thus, since in practice the regions studied often present both regular and irregular zones, an intermediate value of ε is more suitable. Where the point studied coincides with a measurement station, Eq. (14) is not continuous. Continuity is ensured if we assume the measured value at those points.

3.3. Typical meteorological year

At a considered station, the daily global solar irradiation evolution can be represented generating a characteristic year series by means of a typical meteorological year (TMY), which allows us to obtain more accurate results in the simulations [11].

As we can see in the literature, autoregressive moving average (ARMA) models are widely applied to time series [20]. A series can be adjusted by means of an additive method,

$$Y_t = \alpha_0 + \sum_{i=1}^{r} \left[\alpha_i \cos\left(\frac{2\pi\, i\, t}{T}\right) + \beta_i \sin\left(\frac{2\pi\, i\, t}{T}\right) \right] + \epsilon_t \quad t = 1, \ldots, n, \tag{15}$$

where ω is a constant and the random component, ϵ, fits an ARMA model:

$$\epsilon_t = \phi_1 \epsilon_{t-1} + \cdots + \phi_p \epsilon_{t-p} + a_t + \theta_1 a_{t-1} + \cdots + \theta_q a_{t-q}. \tag{16}$$

The model orders are p and q, and its variability depends upon their immediately previous values and a random series, a_t, which satisfies the following:

$$E(a_t) = 0 \qquad V(a_t) = \sigma_a^2 \qquad \mathrm{Cov}(a_t, a_{t-k}) = 0 \quad \forall t, k.$$

We have computed the daily series for a typical meteorological year of some statistical variables such as maximums, means, medians, vairiances and percentiles of 90% and 75%. The TMY for each of those series is obtained using weighted means to smooth the irregular data. Finally, the TMY series has to be fitted to a third-order Fourier series. The trend of the global irradiation behaviour in every location is represented by the median TMY series because means are more susceptible to spurious data.

The model proposed to represent daily time series for radiation is

$$\frac{T_d - Z_{ad}}{s_d} - M = z_{ad}, \tag{17}$$

where $d = 1, \ldots, 365$ and $a = 1, \ldots, A$, with A being the number of years with data. M is the average of all the original values Z_{ad}, s_d is the series variance, and z_{ad} is the residual ARMA series computed using (16).

The median series is

$$M'_d = \mathrm{median}(Z_{ad}) \quad a = 1, \ldots, A \; d = 1, 2, \ldots, 365. \tag{18}$$

The Henderson moving average [12,11] was used:

$$M_d = M_{21} M'_d \quad d = 1, 2, \ldots, 365. \tag{19}$$

3.3.1. Solar radiation model summary

As can be seen in Fig. 3, the clear sky solar irradiance (W/m^2) is calculated for each time step by means of the equations given above. Applying a numerical integration over a period of time to these values, we obtain the clear sky irradiation (J/m^2). To estimate the real sky radiation values, the calculation of the clear sky index, k_c, is needed. Using this index, computed for any location, we can obtain the real sky irradiance and, of course, the real sky irradiation.

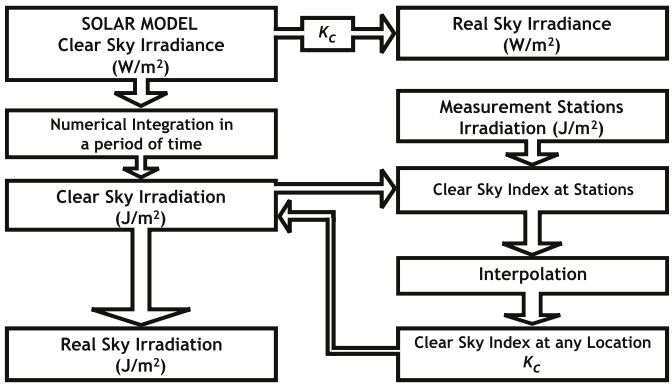

Fig. 3. Solar radiation model outline.

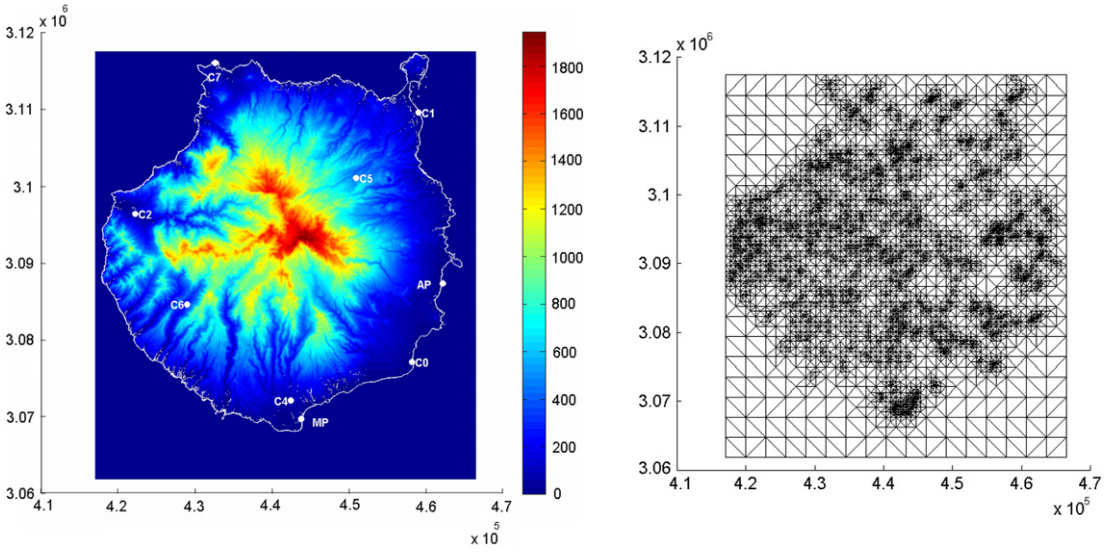

Fig. 4. Elevation (left) and mesh (right) for Gran Canaria Island.

4. Irradiation maps

One of the aims of this paper is to obtain monthly solar radiation maps. Since we are defining the maps for a period of time (a month in our case), the variable to be shown is the irradiation (J/m^2).

In this paper, the maps have been done for Gran Canaria Island (Canary Islands, Spain). The Universal Transverse Mercator (UTM) coordinates (metres) that define the corners of the rectangular domain including the island are (417 025, 3 061 825) and (466 475, 3 117 475), respectively. To define the albedo, the different types of land use in Gran Canaria Island have been studied. In this simulation, the albedo of the zone varies from 0.05 (Macaronesic laurisilva) to 0.6 (salt mine). The locations of the measurement stations[1] for the island are described in Table 1, and in Fig. 4. Starting from the albedo and topography data, we will construct a mesh of triangles that must be adapted to the geographical characteristics of the terrain by using a refinement/derefinement procedure that takes into account elevation and albedo maps simultaneously. Great variations in topography or albedo imply more points to define the mesh, i.e., we will have triangles from a few kilometres (e.g., on the sea) to a few metres (e.g., on steep slopes) of edge length. To obtain good accuracy, we chose $\varepsilon_h = 130$ and $\varepsilon_a = 0.08$, so a mesh with 5866 nodes and 11683 triangles is built to define Gran Canaria Island (see Fig. 4). Once the terrain and albedo characteristics have been modelled by means of a mesh, the solar radiation equations given in Section 3 can be applied. The results obtained for each and every time step of a day (e.g. an hour) need to be weighted by the shadow analysis done in 2.2. For each day, the clear sky global irradiance is computed with the desired time step, as the addition of the three components.

Now that all the irradiance values are calculated for every time step, if we want to know the actual energy that reaches any point of the mesh, we will have to integrate the irradiance, for example, over a day. For this purpose we have used the

[1] Courtesy of the Instituto Tecnológico de Canarias.

Table 1
Geolocations of measurement stations on Gran Canaria Island.

Station	Label	Latitude	Longitude	Height
Pozo Izquierdo	C0	27.8175 N	15.4244 W	47
Las Palmas de G. C.	C1	28.1108 N	15.4169 W	17
La Aldea de San Nicolás	C2	27.9901 N	15.7907 W	197
San Fernando de M.	C4	27.7716 N	15.5841 W	265
Santa Brígida	C5	28.0337 N	15.4991 W	525
Mogán (village)	C6	27.8839 N	15.7216 W	300
Sardina de Gáldar	C7	28.1681 N	15.6865 W	40

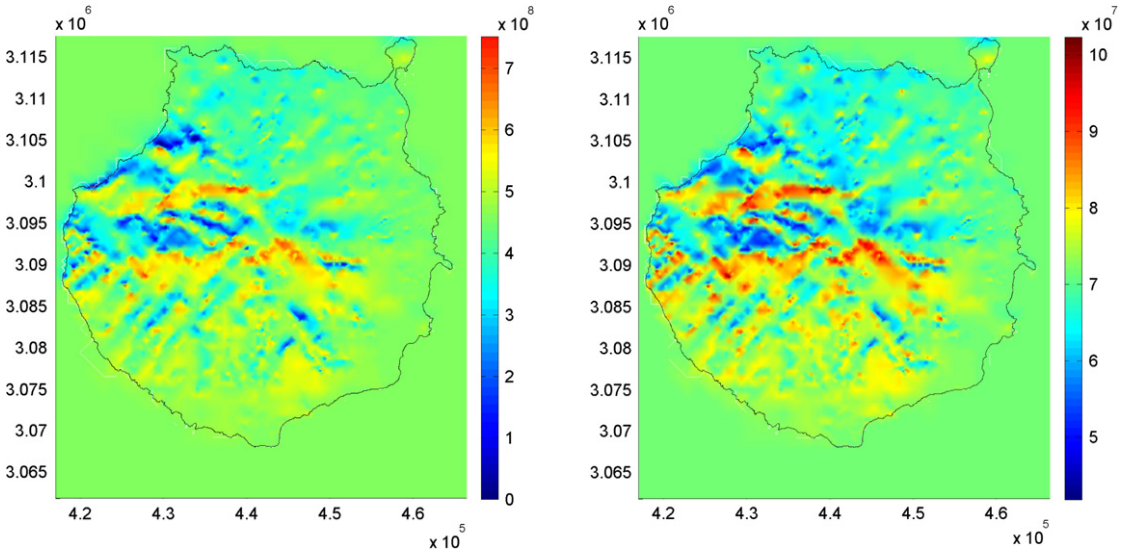

Fig. 5. Beam (left) and diffuse (right) radiation maps (J/m^2) for January (TMY).

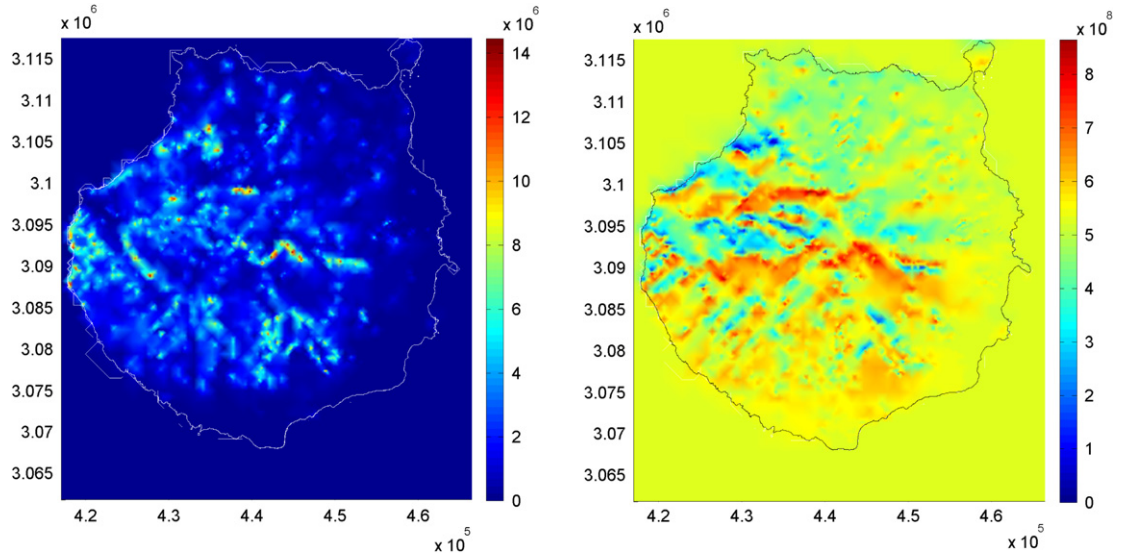

Fig. 6. Reflected (left) and global (right) radiation maps (J/m^2) for January (TMY).

Simpson formula to integrate these data numerically in order to obtain the daily radiations. In Fig. 3 we can see the flow of actions to obtain the daily irradiation values for real sky conditions.

Now we are able to draw an irradiation map for a time period. For example, we can see the irradiation map of Gran Canaria Island for January (TMY), for clear sky conditions. In Fig. 5, beam (left) and diffuse (right) radiation maps (J/m^2) are presented. In Fig. 6, we can see the reflected and global radiation for the same month.

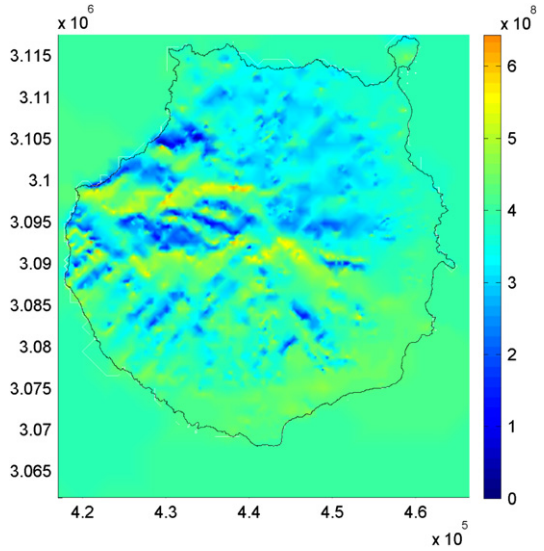

Fig. 7. Global real sky radiation map (J/m^2) for January (TMY).

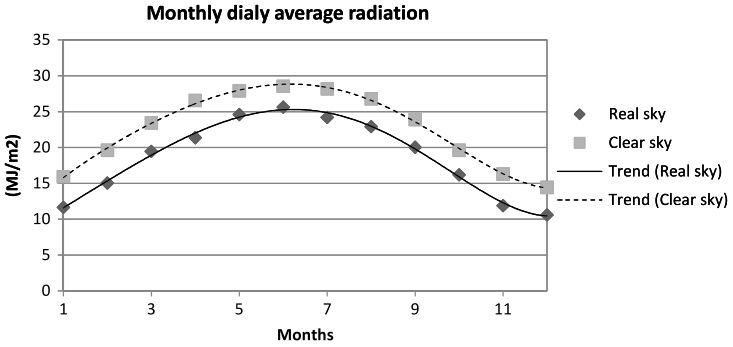

Fig. 8. Monthly average radiation per day.

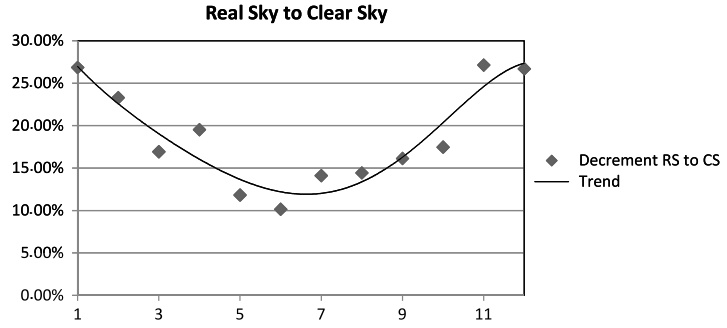

Fig. 9. Percentage decrease in computed radiation.

Fig. 7 shows the global irradiation map for the island under real sky conditions for January. The monthly average real sky global radiation per day, for the whole studied region of the example (Gran Canaria Island), varies from 10.6 MJ/m^2 per day in December, to 25.6 MJ/m^2 per day in June (see Fig. 8). In this figure, we can see the annual evolution of the computed monthly average per day for both clear sky and real sky global radiation.

Taking a look at the differences between both curves, we obtain Fig. 9, where the percentage decrease from the computed radiation is presented. In this figure, we observe the radiation behaviour for our example, where the highest number of clear days occur in Spring, especially during the months of May and June. We can see the typical behaviour of the cloudiness produced by the Trade Winds over the island during Summer. In Fig. 10, we can see the global real sky irradiation maps for the months of April and July (TMY).

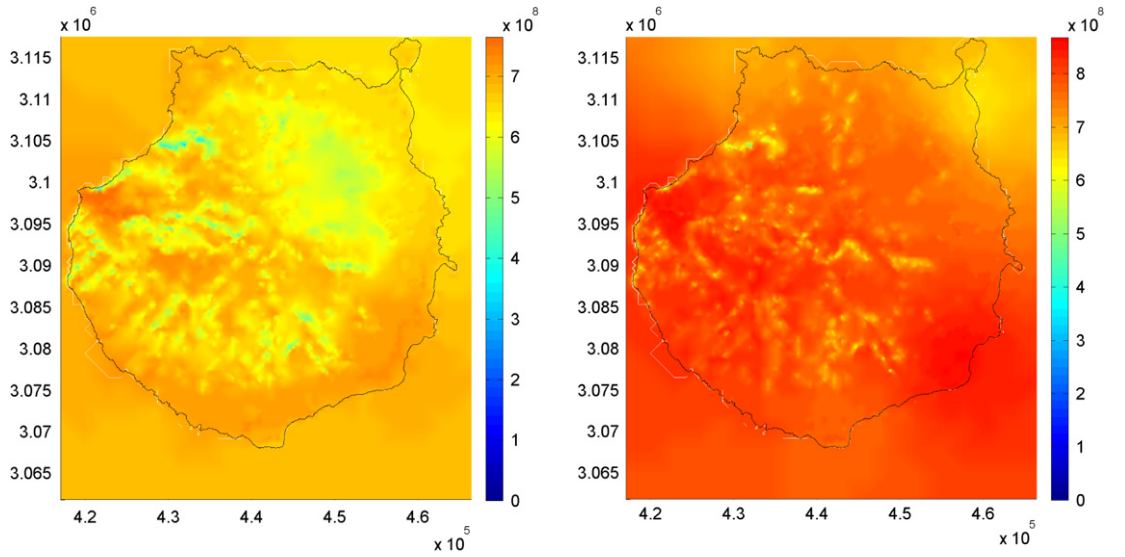

Fig. 10. Global real sky radiation map (J/m^2) for April (left) and July (right).

5. Irradiance graphs

The previous section showed the distribution maps for irradiation as described by ISO 9488, i.e., the radiation energy density that comes into contact with the terrain. However, solar radiation incidence on the terrain varies from zero at dawn up to a maximum at noon, and then decreases until sunset, when it becomes zero again. The irradiation per time unit is the irradiance, usually given in W/m^2. The analysis of irradiance values is of utmost importance when it comes to studying electric power generation through solar radiation conversion. An irradiance graph for a TMY particular day allows us to know the expectable electric power production per hour (or per another time step). This is a big help when trying to make an optimal electric power dispatch in order to have a high solar energy penetration in the electric power system. This fact is increasingly more likely due to the growth of solar power installed, whether it be photovoltaic or solar thermal power. The calculation of the subsequent conversion to electric power is easy, using models of photovoltaic and/or solar thermal power conversion.

The real sky irradiance will be calculated (Fig. 3) using the clear sky index values obtained by means of Eq. (14) and considering a linear distribution along the day. This is done to avoid an extremely high computational cost. If more accuracy is needed, k_c can be calculated for every time step as long as there are available data. In Fig. 11, the irradiances in Maspalomas[2] for clear and real sky are shown for 15 January (left) and 15 July (right). All values are calculated assuming a horizontal surface. The abscissa values are the coordinated universal time (UTC) for Gran Canaria Island, which is around one hour forward with respect to the local solar time. As said above, irradiance graphs allow us to know the evolution of the electric power generated through a photovoltaic or solar thermal conversion. In these cases, the surface that receives the radiation is generally not horizontal. As the objective is to maximize the energy production, photovoltaic panels or solar thermal collectors will have a certain inclination with respect to the terrain in order to get the maximum solar radiation. The optimal inclination depends on the latitude of the zone under study and, of course, on the month, day, and time to be considered.

Due to the great importance of solar energy conversion into electric power, it is necessary to use the model with surfaces inclined with respect the horizontal. The way to achieve this goal is by considering a photovoltaic panel or a solar thermal collector inserted in the terrain mesh by means of two or more triangles with the desired inclination, and then calculate the irradiance over it. That is how Fig. 12 has been obtained. There we can see the daily irradiance for a south-oriented collector in Maspalomas on 15 July with different inclinations and with a time step of 30 min. Maximum irradiance (see Table 2) is obtained with a collector inclination of 10° at 13 UTC (12 solar local time). We note that the panel orientation and inclination corresponding to the maximum irradiance do not imply a maximum daily irradiation. Actually the latter is the result of the integration of the irradiance over a day.

This numerical model allows us to evaluate the irradiance for different orientations and inclinations. As an example, the daily irradiance on a collector inclined 60° and oriented east or west is presented in Fig. 13. The left figure shows the east-oriented collector, and the right figure shows the west-oriented collector. The point studied is in Las Palmas de Gran Canaria (north of the island) and the date is 15 January. It is obvious that both curves are now asymmetrical. The east-oriented panel receives higher irradiance values during the first hours in the morning, with a maximum at 10:30 UTC of 566.3 W/m^2. In

[2] South of Gran Canaria Island, next to C4 Station; see Fig. 4.

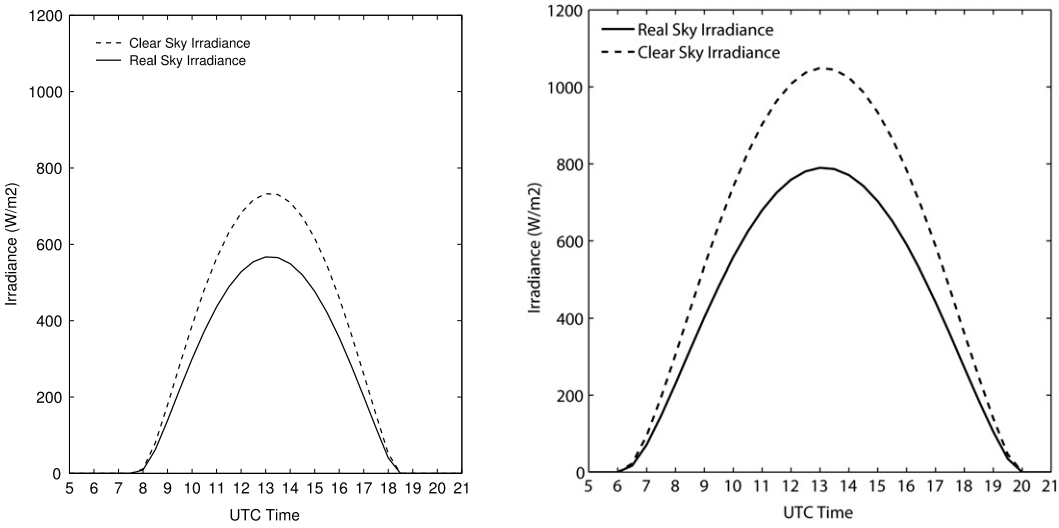

Fig. 11. Daily irradiance (W/m^2) for Maspalomas. January (left) and July (right).

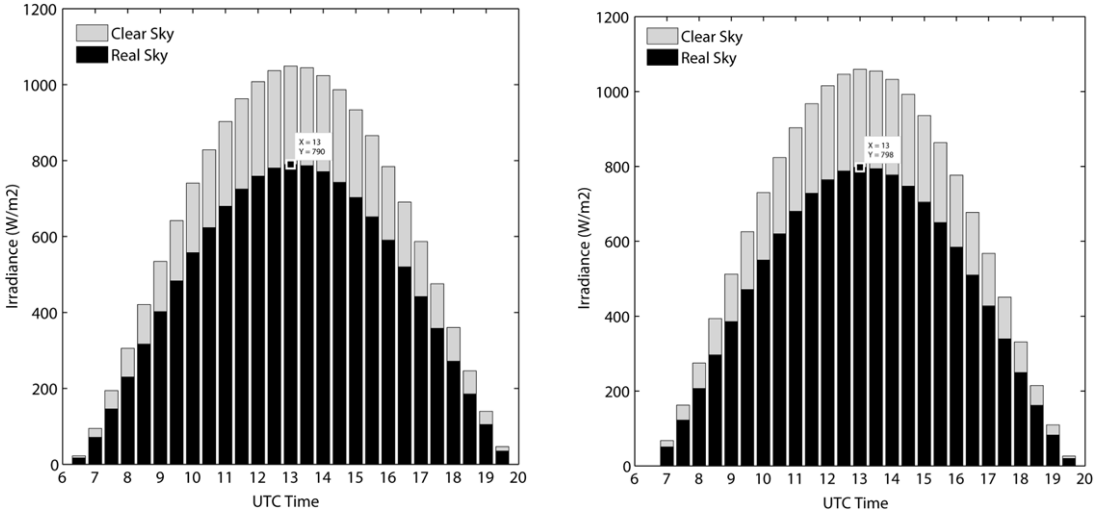

Fig. 12. Daily irradiance for Maspalomas, 15 July. Panel inclination: 0° (left), 10° (right).

Table 2
Maximum irradiance. Maspalomas, 15 July, 13 UTC.

Collector inclination	0°	5°	10°	15°
Irradiance (W/m^2)	790	796	798	795

contrast, the west-oriented panel receives more irradiance during the second half of the day, with a maximum value of 567.8 W/m^2 at 16 UTC.

In the case of photovoltaic or solar thermal power exploitation, especially with high solar energy penetration in the electric power system, an optimal power dispatch is needed. Adjusting the electric power generation to the particular load curve of a system requires knowing the solar power to be generated during the day. The best that can be done in this regard is a prediction of the power generated hour by hour. This prediction would have to be based on a weather forecast that estimates some local weather variables which allow us to know if it is likely to be a cloudy or sunny day at any hour. Therefore, what we need is to adjust the clear sky index k_c hour by hour, to draw an irradiance graph that takes into account the presence of clouds in the hours that they are expected, i.e., to calculate different k_c values depending on the hour.

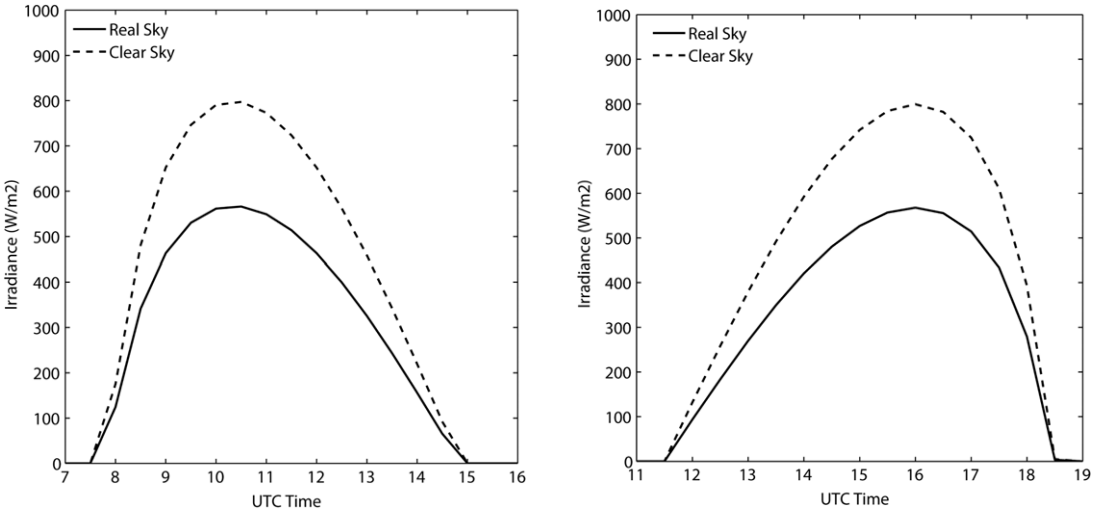

Fig. 13. Irradiance for Las Palmas de Gran Canaria, 15 January. Panel inclination: 60°. Orientation: east (left) and west (right).

6. Conclusions

A numerical model for estimating the solar radiation on a surface is presented. The parameters required are the location, topography, albedo, and observational data. The solar radiation on a surface is estimated by taking into account the shadow distribution in each time step. For this purpose, the adaptivity of the triangulation related to the topography and albedo is essential. Adaptive meshes lead to a minimum computational cost, since the number of triangles to be used is optimum [2].

A typical meteorological year (TMY) [11] is useful for converting the clear sky values into accurate real sky radiation values. To calculate these values, we propose an interpolation method that is suitable when a considerable number of stations are available and they are well distributed in the zone under study. Solar power generation, photovoltaic or solar thermal, can be estimated from real sky values, taking into account the models of the different power station parts. Moreover, rectangular collectors can be included in the model as composed by two triangles in the same plane, with a given inclination and orientation.

The model allows estimating the irradiance for any day (TMY) with the desired time step. This could be a big help in forestry, agronomy, or electrical engineering. It could be an interesting tool with regard to the optimal power dispatch for solar power generation. For this purpose, we need to add meteorological information (for example from models like the MM5, WRF, or HIRLAM) to obtain a predictive solar radiation model.

Acknowledgments

This work has been supported by the *Dirección General de Investigación*, *Ministerio de Economía y Competitividad* of the Spanish Government and FEDER, grant contracts CGL2008-06003-C03-01 and CGL2011-29396-C03-01. The authors also wish to express their sincere thanks to the reviewers, whose comments and suggestions were very helpful.

References

[1] M. Šúri, J. Hofierka, A new GIS-based solar radiation model and its application to photovoltaic assessments, Transactions in GIS 8 (2) (2004) 175–190.
[2] G. Montero, J.M. Escobar, E. Rodríguez, R. Montenegro, Solar radiation and shadow modelling with adaptive triangular meshes, Solar Energy 83 (7) (2009) 998–1012.
[3] F. Díaz, G. Montero, J.M. Escobar, E. Rodríguez, R. Montenegro, A solar radiation model for photovoltaic and solar thermal power exploitation, in: Proceedings of the Seventh International Conference on Engineering Computational Technology, Valencia, Spain, Paper 172, 2010.
[4] A. Niewienda, F.D. Heidt, SOMBRERO: a PC-tool to calculate shadows on arbitrarily oriented sufaces, Solar Energy 58 (4-6) (1996) 253–263.
[5] K. Zakšek, T. Podobnikar, K. Oštir, Solar radiation modelling, Computers & Geosciences 31 (2) (2005) 233–240.
[6] G. Winter, G. Montero, L. Ferragut, R. Montenegro, Adaptive strategies using standard and mixed finite element for wind field adjustment, Solar Energy 54 (1) (1995) 46–56.
[7] L. Ferragut, R. Montenegro, A. Plaza, Efficient refinement/derefinement algorithm of nested meshes to solve evolution problems, Communications in Numerical Methods in Engineering 10 (1994) 403–412.
[8] M.C. Rivara, A grid generator based on 4-triangles conforming. Mesh-refinement algorithms, International Journal for Numerical Methods in Engineering 24 (1987) 1343–1354.
[9] J.W. Gruter (Ed.) Radiation Nomenclature. Brussels, CEC, Second Solar Energy Programme, Project F, Solar Radiation Data, 1984.
[10] M. Blanco-Muriel, D.C. Alarcón-Padilla, T. López-Moratalla, M. Lara-Coira, Computing the solar vector, Solar Energy 70 (5) (2001) 431–441.
[11] L. Mazorra, F. Díaz, G. Montero, R. Montenegro, Typical meteorological year (TMY) evaluation for power generation in Gran Canaria Island, Spain, in: Proceedings of 25th European Photovoltaic Solar Energy Conference and Exhibition, Valencia, Spain, 2010, pp. 4726–4728.
[12] R. Henderson, Note on graduation by adjusted average, Transactions of the Actuarial Society of America 17 (1916) 43–48.
[13] J.K. Page (Ed.), Prediction of Solar Radiation on Inclined Surfaces, D. Reidel Publishing Co., Dordrecht, 1986.

[14] F. Kasten, The Linke turbidity factor based on improved values of the integral Rayleigh optical thickness, Solar Energy 56 (3) (1996) 239–244.
[15] F. Kasten, A.T. Young, Revised optical air mass tables and approximation formula, Applied Optics 28 (1989) 4735–4738.
[16] K. Scharmer, J. Greif, The European Solar Radiation Atlas. Vol. 2: Database and Exploitation Software, Les Presses de l'École des Mines, Paris, 2000.
[17] T. Muneer, Solar radiation model for Europe, Building Services Engineering Research and Technology 11 (1990) 153–163.
[18] T. Muneer, Solar Radiation and Daylight Models for Energy Efficient Design of Buildings, Architectural Press, Oxford, 1997.
[19] G. Montero, R. Montenegro, J.M. Escobar, A 3-D diagnostic model for wind field adjustment, Journal of Wind Engineering and Industrial Aerodynamics 74–76 (1998) 249–261.
[20] R. Aguiar, M. Collares-Pereira, TAG: a time-dependent, autoregressive, Gaussian model for generating synthetic hourly radiation, Solar Energy 49 (3) (1992) 167–174.